

On Integrated Geodetic Monitoring for Sinkhole-Induced Surface Deformation and Mass Dislocation

T. Kersten, L. Timmen, S. Schön

Institut für Erdmessung,

Leibniz Universität Hannover (LUH), Schneiderberg 50, 30167 Hannover, Germany

M. Kobe, G. Gabriel, D. Vogel

Leibniz Institut für Angewandte Geophysik (LIAG), Stilleweg 2, 30655 Hannover, Germany

Abstract Subsidence processes in dense populated urban areas are of societal relevance. SIMULTAN (Sinkhole instability: integrated multi-scale monitoring and analysis) aims at a novel approach to better understand the evolution and characteristics of sinkholes, which are highly correlated with surface deformation. An integrated approach to monitor sinkhole-related mass changes and surface deformations induced by salt dissolution is set up using collocated field sites to combine geodetic and geophysical techniques. Such monitoring sites are established in Hamburg and Bad Frankenhausen (Thuringia). At the latter location, levelling surveys indicate a maximum subsidence rate of max. 4-5 *mm/yr* in the main subsidence areas of Bad Frankenhausen.

This contribution presents a description of the geodetic and geophysical techniques applied, i.e., levelling, GNSS as well as relative/absolute gravimetry. Results from first SIMULTAN campaigns in Bad Frankenhausen are shown.

Keywords. Deformation analysis, Collocated Geo-Monitoring, Sinkhole, Gravity, GNSS

1 Introduction

Sinkholes are circular/elliptical depressions or collapse structures in the Earth's surface, caused by subsion processes, i.e., underground leaching of soluble rocks such as rock salt, anhydrite or limestone. Diameters may range from a few metres to several hundred metres for large sinkholes. Especially in urban areas sinkholes are of societal relevance posing a severe hazard for infrastructure and life. To gain deeper insight into these subsurface processes and related surface deformations, new concepts for monitoring, characterization, and prediction of sinkhole

evolution are required, e.g., a novel combination of geodetic and geophysical techniques. In Northern Germany and Thuringia the development of sinkholes is often related to salt structures, whereas in Central and Southern Germany the soluble rocks are mostly carbonates as indicated by Fig. 1, (Dahm et al., 2010; Schmidt et al., 2012). In Thuringia (Germany) about 20-50 new sinkholes are reported every year.

The interdisciplinary project SIMULTAN (*Sinkhole instability: integrated multi-scale monitoring and analysis*) aims to develop and apply an early recognition system of sinkhole instability, unrest

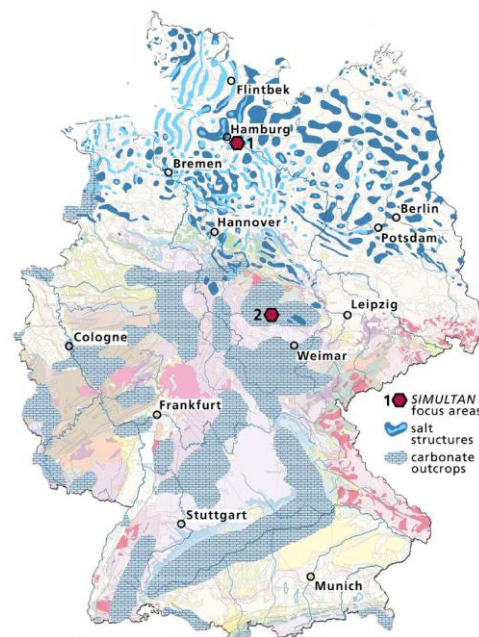


Fig. 1: Simplified geological map of Germany to identify regions of increased sinkhole hazard potential. Soluble rocks are commonly salt and carbonates. The two focus areas of the project SIMULTAN are also shown (after Krawczyk et al. 2015).

and collapse by a rigorous combination of geodetic and geophysical techniques. Research has to be performed on different scales concerning time, lateral extent and depth, (Krawczyk et al., 2015). SIMULTAN will focus on aspects like the separation of different superimposing processes and the understanding of interactions between surface and subsurface as well as the prediction of future sinkhole development and the assessment of damage potential.

Sinkholes either collapse abruptly, thus, forming steep holes (like in Rottleben, Schmalkalden, and Tiefenort/Thuringia) or are continuously subsiding and result in rather flat surface depressions, e.g., in Hamburg-Flottbek or in Ochtmissir Kirchsteig (Lüneburg). Controlling factors are the geological structure and the specific generation process as summarised in Waltham et al. (2005).

Two areas representing evaporitic sinkhole formation are in the focus of SIMULTAN (hexagons in Fig. 1). The first area is Hamburg-Flottbek, a dense populated area which is locally subsiding slowly due to leaching of a salt diapir. The second focus area is Bad Frankenhausen (Thuringia, Germany, sinkhole diameters some tens of metres), which is discussed in more detail in this contribution.

Most of the geological underground of Thuringia is characterised by Permian deposits. Bad Frankenhausen is situated directly south of the Kyffhäuser mountain range at the Kyffhäuser Southern Margin Fault, which is one of the main pathways for circulating ground- and meteoric waters, leaching the Permian deposits, especially the Leine, Staßfurt and Werra formations. Consequently, several sinkholes developed along the Kyffhäuser Southern Margin Fault and still nowadays processes are ongoing. In Bad Frankenhausen precise levelling revealed vertical deformations of 40 mm within 10 years and more than 10 mm between 2014 and 2015 in the area around the oblique spire. However, in both focus areas Hamburg-Flottbek and Bad Frankenhausen the spatio-temporal resolution of surface deformation is still sparse and an integrated interpretation of the data is still missing. Within SIMULTAN geodetic monitoring is performed in close cooperation between the Leibniz Institut für Angewandte Geophysik (LIAG) and the Institut für Erdmessung (Leibniz University Hannover, LUH). The integrated approach comprises gravimetry, levelling and GNSS (GPS - Global Positioning

System and GLONASS - GLobalnaya Navigatsionnaya Sputnikovaja Sistema; Russian pendant to GPS) campaigns.

This paper summarises the layout and first results of this integrated multi-technique deformation monitoring in Bad Frankenhausen. A similar combination of methods has already been designed and established in Hamburg-Flottbek.

2 Concept and Monitoring Strategy

Surface deformation often consists of superimposed signals from several sources at different depths. Combining classical geodetic methods and geophysical strategies, e.g., borehole extensometers in combination with levelling, gravimetry, and GNSS, can provide complementary information and allows discerning between these sources, (NAM, 2000; Rajiyowiryono, 1999).

In SIMULTAN a novel combination of geodetic and geophysical methods will be developed to monitor surface deformation and mass dislocation in the subsurface. Precise GNSS and levelling campaigns together with gravimetric measurements are combined at collocated points to study long periodic effects caused by sinkholes that might be superimposed by seasonal effects. The use of the terminus *integrated* is to understand as a system characterisation for achieving an improved comprehensive solution from the joint interpretation of different kind of results. Thus, collocated points or stations are established, on which measurements with different sensors are performed.

2.1 Design of collocated points

The combination of geodetic and geophysical methods requires an observation network, which is accessible for each of the used methods. Therefore, the planning, selection, and installation of measurement points must be done with great care. In Bad Frankenhausen they are located in active subsidence areas, e.g., around the oblique spire,

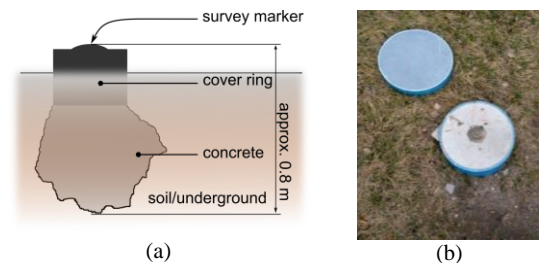


Fig. 2: Schematic sketch of the installation of some collocated points in Bad Frankenhausen, exemplarily for point GRAV12.

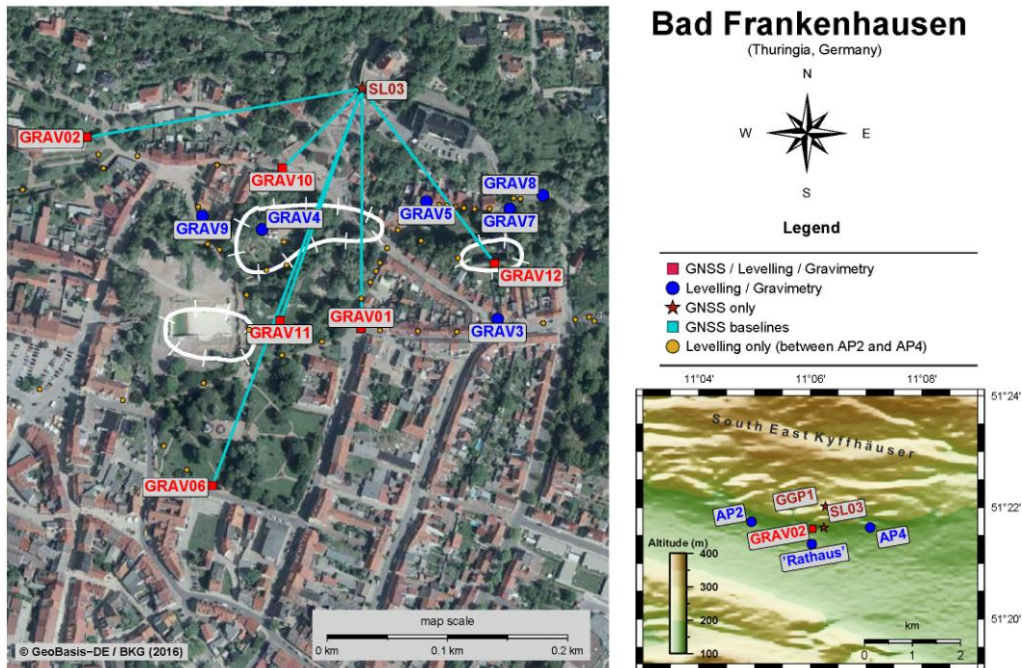


Fig. 3: Location of GNSS and collocated points as part of the geodetic monitoring network in Bad Frankenhausen; white bordered areas indicate regions of sinkhole events.

historical sinkholes, and in assumed stable areas to obtain clear evidence of gravity changes and vertical movements due to subsidence. The gravimeter stations GRAV2, GRAV11 and GRAV12, installed in January 2014, are cast concrete pillars to reduce the influence of micro-seismic noise. They have a diameter of 0.30 m, a depth of 0.8 m and a flat surface with north arrow (Fig. 4). All other points are marked by 0.25 m long stainless steel tubes with a white cap and a fillister head.

2.2 Design of Monitoring Network

The monitoring network in Bad Frankenhausen consists of about 120 points for precision levelling. 13 of these points define a local gravimetric network (Fig. 3) with two more gravity stations outside the city serving as distal reference points. Precise levelling and gravimetric campaigns are conducted quarterly since March 2014 to gain time-lapse datasets in a region characterised by subsidence. An absolute gravimeter point as part of the control network has been established in 2015 to monitor the long-term stability of the gravity reference and, thus, to identify regional gravity changes related to subsidence over several years or even decades. This point is reoccupied annually. The complete GNSS part of this multi-sensor monitoring network consists of six collocated points (combination with gravimetry, Fig. 3) plus

two additional sites (GGP1, SL03), where only GNSS is observed. Station SL03 serves as a local reference for the GNSS network. GNSS campaigns started in September 2015 and will be repeated every six months at the same time as the gravimeter and levelling campaigns. Furthermore, a borehole extensometer is installed at point GRAV7 and operated by the Geological Survey of Thuringia.

The integrated study in SIMULTAN comprises the monitoring at collocated points in quarterly (gravimetry, levelling) and semi-annually (GNSS) field campaigns, as well as the combination and integration of the results of the different monitoring techniques and their interpretation as an integrated solution.

3 Levelling and Gravimetry Campaigns

3.1 Geometric Levelling

The levelling network of about 120 points is established to observe subsidence in the northern area of the city and to provide evidence for measuring campaigns using GNSS. Furthermore, levelling supports the processing and interpretation of the gravity data by providing heights and height changes for different processing steps, e.g., further gravity anomaly calculation.

Levelling campaigns are performed with a Leica Geosystems digital levels DNA03 and bar code invar staffs (accuracy after manufacturer information ± 0.3 mm per 1 km double levelling).

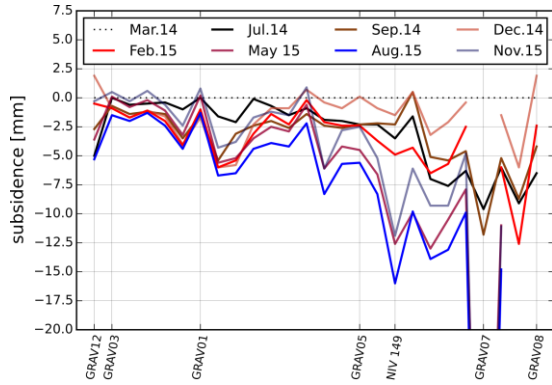


Fig. 4: Subsidence from March 2014 (baseline reading) to November 2015 obtained from quarterly performed precise levelling. Graphs are based on all levelling points along a profile, starting at GRAV12 and ending at GRAV8 (Fig. 3). At GRAV7 subsidence amounts to ca. 70 mm, but is expected to be partially induced by construction work.

The standard deviation for one km of double levelling is in the range of 1.5 mm or less in each of the eight field campaigns. Furthermore, the results reveal a maximum subsidence rate of around 4-5 mm/yr in the main subsidence area since 2014 (Fig. 4; GRAV1 to GRAV5). The significantly higher values observed at the points GRAV5 and GRAV8 can in parts possibly be explained by compaction of the soil due to extensive construction work, e.g., a research drilling near point GRAV7. It is not possible yet to separate these effects from long-term, subsrosion-induced subsidence.

3.2 Gravimetry

A good overview about relative and absolute gravity is given by Timmen (2010). Relative gravimetry in Bad Frankenhausen is carried out in field campaigns together with the precise levelling. During every campaign four different gravimeters of the types Scintrex CG3, CG5, and LaCoste & Romberg (LcR) are used to optimise the network surveys. In total, 15 gravity stations (13 local and 2 distant reference points) are observed using the step method for drift control of the spring gravimeters, (Torge and Müller, 2012).

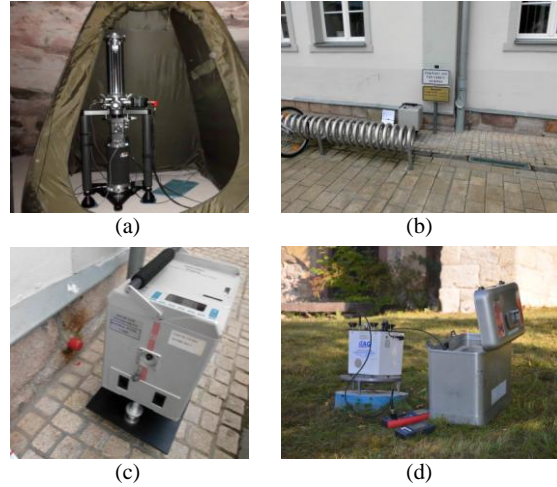


Fig. 5: Relative and absolute gravimeter measurements at Bad Frankenhausen. Absolute gravity value determined with FG5X-220 in cellar vault (a), determination of gravity tie from absolute to relative point using levelling mark as survey station (b, c) and relative measurements with LaCoste-Romberg (LcR) on GRAV12 (d).

First data processing includes the elimination of outliers, jumps, and other failures in the data sets as well as the reduction for earth tides, instrumental drifts, instrument heights, and air pressure changes. Moreover, calibration factors and sealing of the instruments are checked regularly. Inside the local observation area the maximum gravity difference is $44.5 \mu\text{m/s}^2$ between the points GRAV4 and GRAV12. Hence, a calibration accuracy of better than 10^{-3} ($\approx 0.0445 \mu\text{m/s}^2$) is needed to avoid a significant systematic effect on the whole network. The obtained standard deviations of the gravity points in each campaign are in the order of less than $0.02 \mu\text{m/s}^2$ (Scintrex), $0.05\text{-}0.07 \mu\text{m/s}^2$ (LCR), and for a combined adjustment of the data from all gravimeters in the order of $0.015 \mu\text{m/s}^2$ or even better.

The absolute gravimeter point was established in Bad Frankenhausen in June 2015 to determine and control the absolute gravity level (datum) for the relative gravimetry campaigns. The absolute gravity point is located in the cellar of the town hall of Bad

Tab. 1: Results of the absolute gravity campaign with the gravimeter FG5X-220 on the “Rathaus” point (cellar vault, Fig.4); s: standard deviation.

Site Rathaus	Measurement run (orientation)	Date in 2015	Drops	$\delta g/\delta h$ [$\mu\text{m/s}^2 / \text{m}$]	$g_{h=1.250}$ [$\mu\text{m/s}^2$]	$g_{h=0.000}$ [$\mu\text{m/s}^2$]
Setup 1	20150622a (N)	22./23. June	998	-2.678	9811717.488 s=0.001	
Setup 2	20150623a (W)	23./24. June.	798	-2.678	9811717.458 s=0.001	
Average		22.–24. June.	1796	-2.678	9811717.473	9811720.820

Frankenhausen. Measurements were performed by LUH using the Hannover absolute gravimeter FG5X-220 (ref. Fig. 5(a)). This gravimeter participated in the latest international comparisons (Walferdange, Luxembourg, Nov. 2013 and Belval, Luxembourg, Nov. 2015) and agrees within $0.02 \mu\text{m/s}^2$ with the international realised measuring level, (Timmen et al., 2015). The absolute gravity campaign in Bad Frankenhausen consists of 998 drops in the first and 798 drops in the second setup (50 drops/set). The results are shown in table 1. Earth tides as described by Timmen and Wenzel (1995) were reduced. Air pressure induced gravity changes were considered by applying the correlation factor -3.0 nm/s^2 per hPa . The gradient insensitive sensor height, also known as dead-gradient-point, depends on the gravimeter setup and is close to 1.25 m above floor level. Thus, the reference height $h=1.250 \text{ m}$ (above floor point) is chosen for comparison reasons. The applied vertical gradient is assumed to be constant along the plumb line at this point and, because of the chosen reference height, the effect of its uncertainty on the absolute value can be neglected. The gradient $\delta g/\delta h$ was measured with Scintrex CG3M-4492 of LUH between the sensor positions 0.251 m and 1.165 m above floor point. The observed gravity gradient is determined to $-2.678 \mu\text{m/s}^2$ per m with a standard deviation of $0.009 \mu\text{m/s}^2$ per m . To combine absolute and relative gravimetric measurements, the centred g -value ($h = 0.0 \text{ m}$) is provided in table 1. The gravity tie between the absolute gravity point in the basement of the town hall to the outdoor point in front of the town hall, which is the starting point for relative measurements, is determined using the Scintrex CG3M meter of LUH. The Δg -value between the absolute and relative point (wall bolt, Fig. 5(c)) has been determined with $\Delta g = -4.631 \mu\text{m/s}^2$ and a standard deviation of $\sigma_{\Delta g} = 0.015 \mu\text{m/s}^2$. The reference height of the Δg result is set to the top of the wall bolt or levelling bench mark, respectively.

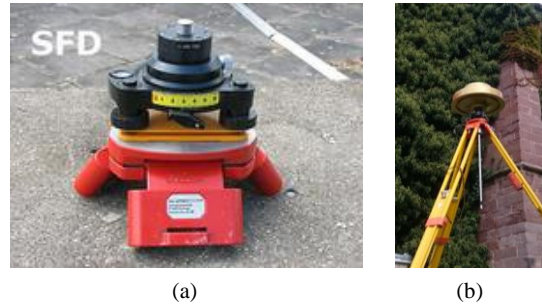


Fig. 6: GNSS adaptor for precise GNSS height levelling, (a) mockup for calibration on robot and (b) installation in the field with 50 cm scale beneath the ARP exemplarily shown for point GRAV12.

4 GNSS campaigns

For consistent monitoring, equal and close similar GNSS receivers are used. Local reference stations and challenging stations are equipped with 3d choke ring antennas (Leica AR25 Rev. 3) to mitigate most of expectable multipath and to capture observation with optimal antenna gain especially at low elevation. Other stations are equipped with rover antennas (Javad GrAnt G3T) for economical reasons. The GNSS equipment is summarised in table 2.

The highest accuracy is only attainable, if GNSS-inherent errors are modelled properly. Therefore, all used GNSS antennas are calibrated absolutely at the LUH facility using the robot based approach, (Wübbena et al., 1996; Seeber and Böder, 2002). Since the height component is – in addition to the horizontal components – of particular interest, the special tripod adaptor FG-ANA100B as shown in Fig. 6 is used in SIMULTAN campaigns. Such adaptors are widely used in high precision GNSS levelling surveys as, e.g., described in Hirt et al. (2011). The adaptor contains a 0.5 m scale, directly connected to the antenna reference point (ARP) to support precise determining of the antenna height during GNSS sessions by levelling. Heights are controlled several times during each session.

Tab. 2: GNSS equipment used in SIMULTAN campaign

Element	IGS Note	Serial number	Used System
Receiver	LEICA GRX1200+GNSS	5035	GPS/GLO/GAL/BDS
	LEICA GRX1200+GNSS	5791, 5883	GPS/GLO/GAL
	LEICA GX1230GG	1887	GPS/GLO
	LEICA GRX1200GG Pro	6640	GPS/GLO
Antenna	LEIAR25.R3 NONE	8360002, 8420013	GPS/GLO/GAL/BDS
	JAVGRANT-G3T NONE	3451, 3447, 3486	GPS/GLO/GAL/BDS

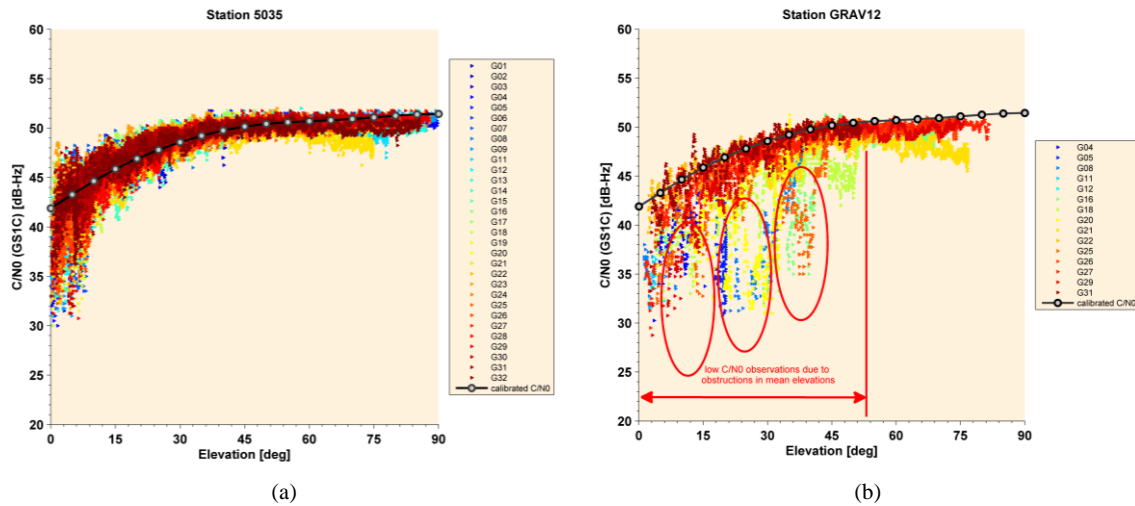


Fig. 7: Carrier-to-noise density ratio (C/N0) as signal quality indicator, (a) Determination of a nominal behaviour at the laboratory network of LUH, and (b) observed C/N0 in Bad Frankenhausen with the same antenna/receiver combination but influenced by urban reflectors.

4.1 Session setup

Each SIMULTAN GNSS campaign consists of three sessions with observation time of four hours. Data is captured with a 1 second interval but is reduced to 15 seconds for the final GNSS network analysis and adjustment.

For the GNSS network, a stable and reliable point is mandatory to realise the geodetic datum. Point SL03 meets the requirements since it is installed on a concrete pillar with well defined centring. Together with station GRAV11 the point SL03 (indicated by a red star in Fig. 3) is continuously observing during all 6 sessions. A star like network is formed with baselines starting at SL03. The GNSS stations indicated by a square symbol in Fig. 3 are occupied only during three sessions.

4.2 Campaign preparation

Concerning GNSS, SIMULTAN includes two challenging tasks. On the one hand high precision estimates of the horizontal and vertical coordinate have to be achieved to precisely determine deformations in the three dimensions. On the other hand urban environment is challenging for GNSS signals due to signal obstructions, multipath and diffractions. An intensive station selection and analysis verified moderate obstructions in the receiving antenna's field of view for all selected GNSS points. In further analysis adaptive and dynamical obstructions masks will be studied and applied in SIMULTAN to further improve the signal availability.

A zero baseline (ZB) test at the laboratory network of LUH was carried out to examine the used GNSS receivers and control them against each other. In this experiment, all receivers were connected to a unique Leica AR25 Rev 3 antenna. Data is captured and evaluated on two important indicators:

- 1 Study of the achievable carrier-to-noise ratio (C/N0) for receiver-antenna combination under ordinary campaign settings, cf. Fig. 7, (Brunner et al., 1999)
- 2 Analysis of double differences (DD) between the individual receivers.

Based on the ZB setup, the DDs show an expected noise level with maximal peak to peak variations of $\pm 3.5-4 \text{ mm}$. No suspicious observations and behaviours of several receivers were found. Thus, the correct functionality of the receivers is verified. The C/N0 values are adequate for quantifying the signal quality. Following Brunner et al. (1999), C/N0 reference curves are necessary to describe the nominal behaviour of the receiver-antenna combination. Reference curves can be evaluated using moderate amount of satellite observations in a static approach with few obstructions (ref. Fig. 7(a)) or by antenna calibration with a robot, (Rao, 2013). Fig. 7(a) summarizes C/N0 values for all measured satellites during 24 hours w.r.t the elevation in the antenna's body frame. At elevations between $30^\circ-90^\circ$ stable C/N0 of 54 dB-Hz could be detected. At elevations lower than 30° , C/N0 of 40 dB-Hz are observed. In addition to Fig 7(a), where a typical C/N0 curve from the ZB test is shown, Fig 7(b) shows C/N0 values of a four hours session at point GRAV12. For observations below 45° , elevation

bins with large C/N0 deviation from the nominal curve (black line) can be seen. These effects are due to signal diffraction and subsequently distorted carrier phase observations.

Processing of precise GNSS single station solution and network adjustment is carried out using Bernese 5.2 with CODE products e.g. clock, orbits, earth rotation parameters or differential code biases, (Dach et al., 2015).

For an advanced station analysis and the study of the application of dynamic and adaptive elevation masks, a GNSS Matlab Toolbox, developed at LUH, is used in addition, (Weinbach and Schön, 2011).

4.3 Local reference and network solution

The approximate coordinates of the local reference station SL03 were determined using Precise Point Positioning (PPP) with sidereal repetition, (Zumberge et al. 1997) including necessary models like, e.g., atmospheric corrections, (Blewitt 2003). Figure 8 lists the individual solutions and corresponding residuals w.r.t. the mean. The first two sessions (279-0 and 279-1, year 2015) are based on four hours of observation and sessions 280-0 and 281-0 based on nine hours. Homogeneous repeatability of less than 3.5 mm in horizontal and height component is obtained, although the equipment had to be removed every day.

The network processing was evaluated using both, a GPS only and a GPS/GLONASS combined solution, to study the impact on the network performance.

In Tab. 3 first results of the network solutions are summarised. The results show that a combined solution is much more reliable and improves the repeatability for the horizontal and especially the height component. Gaining an optimal estimate for the up component is challenging due to several urban reflectors and obstructions. Here, the

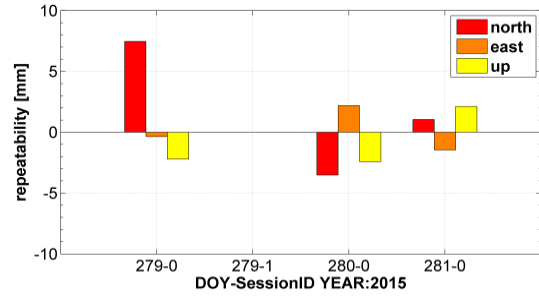


Fig. 8: Comparison of individual PPP solutions obtained during campaign to define local reference station.

advantage of using adaptive and dynamic elevations masks will reduce the problem, so that satellite arcs with interrupted and disturbed observations can be identified and reduced to a minimum.

The improved repeatability especially for the height component is the result of combining GPS and GLONASS. One advantage is that GLONASS supports satellites with a higher elevation, so that especially the northern hole (characteristic in mid-latitudes) can be reduced. Furthermore, the doubled amount of observations stabilises the result additionally.

5 Summary and Outlook

First results from the SIMULTAN campaigns to monitor sinkholes in Bad Frankenhausen are shown. The presented network in Bad Frankenhausen consists of 120 levelling points 15 of these points are used as a relative gravimetric measurement network, whereof six points are additionally occupied by GNSS. The first multi-sensor monitoring campaigns have been performed. Quarterly levelling confirms a subsidence rate of 4-5 mm/yr in the main subsidence areas of Bad Frankenhausen. The gravity network covers a gravity range of 44.5 $\mu\text{m/s}^2$ between the points GRAV4 and GRAV12 and has been observed in quarterly campaigns. The standard deviations of single gravity points in each campaign are in the

Tab. 3: GPS-only and combined GPS/GLONASS network solution using L1 Signal for SIMULTAN monitoring network.

No	Station	RMS			RMS		
		GPS only [mm]			GPS+GLO [mm]		
		north	east	up	north	east	up
1	GGP1	2.01	5.26	8.96	1.00	4.40	6.70
2	GR01	0.52	1.19	0.30	1.74	0.81	1.67
3	GR02	0.39	4.28	11.44	0.49	3.98	6.40
4	GR06	0.91	5.11	12.55	0.58	4.79	7.83
5	GR10	1.09	1.59	3.78	0.29	1.34	0.98
6	GR11	1.23	2.87	7.16	0.79	2.19	8.22
7	GR12	0.45	3.16	4.62	0.64	0.71	0.98

order of $\leq 0.015 \mu\text{m/s}^2$ for a combined adjustment of all available data. In addition, annual monitoring of the absolute gravity reference has been initiated by LUH using the FG5X-220 free-fall gravimeter in 2015.

Finally, combined GPS/GLONASS campaigns (six-monthly) are evaluated. Contrary to GPS only, they provide more reliable estimates for the horizontal and height component of 2-3 mm for optimal points and 6 mm in the horizontal components and 12 mm in the height component for challenging stations.

Urban sites are challenging for all kind of used measurement techniques but show that reliable solutions are feasible. Further campaigns will be conducted to achieve an improved understanding of land subsidence.

Acknowledgment

The authors like to thank the SAPOS team of the TLVerm Thuringia, the Glückauf Vermessung GmbH Sondershausen, and the staff of the city of Bad Frankenhausen for the kind cooperation. Furthermore, the authors like to thank the LGLN (Lower Saxony) for providing additional FG-ANA100B GNSS height adaptors and corresponding accessories. CODE is thanked for providing freely GNSS products. SIMULTAN is funded by the Federal Ministry of Education and Research based on a resolution by the German Bundestag.

References

Blewitt, G., 2003. Self-consistency in reference frames, geocenter definition, and surface loading of the solid Earth. *Journal of Geophysical Research*, February, 108(B2, 2103), p. 10.

Brunner, F.K., Hartinger, H., Troyer, L. 1999. GPS signal diffraction modelling: the stochastic SIGMA-d model, *Journal of Geodesy*, 73, pp. 259-267.

Dach, R., Lutz, S., Walser, P. and Fridez, P. eds., 2015. *Bernese GNSS Software Version 5.2*. University of Bern.

Dahm, T., Kühn, D., Ohrnberger, M., Kröger, J., Wiederhold, H., Reuther, C.-D., Dehghani, A. and Scherbaum, F., 2010. Combining geophysical data sets to study the dynamics of shallow evaporites in urban environments: application to Hamburg, Germany. *Geophysical Journal International*, 181(1), pp. 154-172.

Hirt, C., Schmitz, M., Feldmann-Westendorff, U., Wübbena, G., Jahn, C.-H. and Seeber, G., 2010. Mutual validation of GNSS height measurements and high-precision geometric-astronomical leveling. *GPS Solutions*, 15(2), pp. 149-159.

Krawczyk, C. M., Polom, U. and Bunes, H., 2015. Geophysikalische Schlüsselparameter zur Überwachung von Erdfällen – Stand und Ziele der aktiven Seismik. In: Deutsche Geophysikalische Gesellschaft (edt.): DGG

Kolloquium Georisiken – Erdfälle, DGG Mitteilungen, Sonderband I/2015, pp. 19-29.

NAM, 2000. *Bodemdaling door Aardgaswinning Groningen veld en randvelden in Groningen, Noord Drenthe en het Oosten van Friesland - Status Rapport en Prognose tot het jaar 2050*. Nederlandse Aardolie Maatschappij BV, p. 25.

Rajiyowiryono, H., 1999. Groundwater and land subsidence monitoring along the north coastal plain of Java island. *CCOP Newsletter*, 24(3), p. 19.

Rao, B. R., Kunysz, W., Fante, R. L. and McDONALS, K., 2013. *GPS/GNSS Antennas*. Artech House Publishers, Norwood, USA.

Schmidt, S., Wunderlich, J., Geletneky, J. and Steinborn, H., 2012. Untersuchungen und Maßnahmen am Erdfall Tiefenort, Frankensteinststraße, im Nachgang des Erweiterungsbruches vom 28. 01. 2010 - Gefährdungsanalyse am Inneren Salzhang Tiefenort. *Unveröff. Ergebnisbericht, Thür. Landesanst. f. Umwelt und Geologie*, p. 151.

Seeber, G. and Böder, V., 2002. Entwicklung und Erprobung eines Verfahrens zur hochpräzisen Kalibrierung von GPS Antennenaufstellungen - Schlussbericht zum BMBF/DLR Vorhaben 50NA9809/8. *Institut für Erdmessung*, p. 71.

Timmen, L. 2010. Absolute and relative Gravimetry. In: Xu, G. (ed) *Sciences of Geodesy – I*, chapter 1, Springer, Berlin, pp. 1-48.

Timmen, L., Engfeldt, A. and Scherneck, H.-G., 2015. Observed secular gravity trend at Onsala station with the FG5 gravimeter from Hannover. *Journal of Geodetic Sciences*, 5(1), pp. 18-25.

Timmen, L. and Wenzel, H.-G., 1995. Worldwide synthetic gravity tide parameters. In: H. Sünnkel and I. Marson, (eds.): *Gravity and Geoid*, Proc. IAG Symp., Springer Berlin Heidelberg, pp. 92-101.

Torge, W. and Müller, J., 2012. *Geodesy*. 4 ed. De Gruyter, Berlin/Boston.

Waltham, T., Bell, F. G. and Culshaw, M., 2005. *Sinkholes and Subsidence*. Springer. p. 350.

Weinbach, U. and Schön, S., 2011. GNSS receiver clock modeling when using high Precision oscillators and its impact on PPP. *ASR*, 47(2), pp. 229-238.

Wübbena, G. Menge, F., Schmitz, M., Seeber, G., Völksen, C. 1996. *A New Approach for Field Calibration of Absolute Antenna Phase Center Variations*. In: Proceedings of the 9th International Technical Meeting of the Satellite Division of the Institute of Navigation (ION GPS), September 17-20, Kansas City, pp. 1205-1214.

Zumberge, J. F. et al., 1997. Precise Point Positioning for the efficient and robust analysis of GPS data from large networks. *Journal of Geophysical Research*, 102(B3), pp. 5005-5017.